THE EUROPEAN
PHYSICAL JOURNAL PLUS

Regular Article

Spectrum of strange singly charmed baryons in the constituent quark model

Keval Gandhi[a], **Ajay Kumar Rai**[b] [iD]

Department of Applied Physics, Sardar Vallabhbhai National Institute of Technology, Surat, Gujarat 395007, India

Abstract Excited-state masses of the strange singly charmed baryons are calculated using the nonrelativistic approach of the hypercentral constituent quark model. The hyper-Coulomb plus screened potential is used as a confinement potential with the first-order correction. The spin–spin, spin–orbit and spin–tensor interaction terms are included perturbatively. Our calculated masses are allowed to construct the Regge trajectories in both (n_r, M^2) and (J, M^2) planes. The mass spectra and the Regge trajectories study predict the spin–parity of $\Xi_c(2970)^{+/0}$, $\Xi_c(3080)^{+/0}$, $\Xi_c(3123)^+$, $\Omega_c(3000)^0$ and $\Omega_c(3119)^0$ baryons. Moreover, the strong one-pion decay rates of the isodoublet states of $\Xi_c(2645)$, $\Xi_c(2790)$ and $\Xi_c(2815)$ are analyzed in the framework of heavy hadron chiral perturbation theory. Also, the ground-state magnetic moments and the radiative decay rates based on the transition magnetic moments are calculated in the framework of the constituent quark model.

1 Introduction

The strange singly charmed baryons Ξ_c and Ω_c^0, respectively, belong to the antisymmetric antitriplet and symmetric sextet SU(3) flavor representations. Recently, the particle data group (PDG) listed the nine baryonic states of Ξ_c baryon: $\Xi_c(2470)^{+/0}$, $\Xi_c(2645)^{+/0}$, $\Xi_c(2790)^{+/0}$, $\Xi_c(2815)^{+/0}$, $\Xi_c(2930)$, $\Xi_c(2970)^{+/0}$, $\Xi_c(3055)^+$, $\Xi_c(3080)^{+/0}$, $\Xi_c(3123)^+$; and the six of Ω_c^0 baryon: $\Omega_c(2770)^0$, $\Omega_c(3000)^0$, $\Omega_c(3050)^0$, $\Omega_c(3065)^0$, $\Omega_c(3090)^0$ and $\Omega_c(3120)^0$ (shown in Table 1) [1]. The masses, isospin mass splitting, spin–parity, decay widths, lifetime, etc., of these baryons were measured by the ARGUS, CLEO, E687, FOCUS, $BABAR$, Belle, CDF and LHCb experimental collaborations. The comprehensive review articles wrote detailed information on singly charmed baryons [2–4]. Moreover, the present experimental facilities Belle II, LHCb, J-PARC and the upcoming experiment $\overline{P}$ANDA [5–10] are expected to study singly heavy hadrons in the near future.

Experimentally, the ground-state mass spectra of strange singly charmed baryons are now well established and many new excited states were found in the past few years. The $BABAR$ detector measured the mass and the decay width of $\Xi_c(2930)$ [11]. Reference [12] observed two new resonances $\Xi_c(3055)^+$ and $\Xi_c(3123)^+$ decaying into $\Sigma_c(2455)^{++}K^-$

[a] e-mail: keval.physics@yahoo.com

[b] e-mail: raiajayk@gmail.com

Table 1 Mass, width and J^P value of the strange singly charmed baryons from PDG [1]

Resonance	Mass (MeV)	Width (MeV)	J^P
Ξ_c^+	2467.87 ± 0.30	–	$\frac{1}{2}^+$
Ξ_c^0	$2470.87^{+0.28}_{-0.31}$	–	$\frac{1}{2}^+$
$\Xi_c'^+$	2578.4 ± 0.5	–	$\frac{1}{2}^+$
$\Xi_c'^0$	2579.2 ± 0.5	–	$\frac{1}{2}^+$
$\Xi_c(2645)^+$	2645.53 ± 0.31	2.14 ± 0.19	$\frac{3}{2}^+$
$\Xi_c(2645)^0$	2646.32 ± 0.31	$2.35 \pm 0.18 \pm 0.13$	$\frac{3}{2}^+$
$\Xi_c(2790)^+$	2792.0 ± 0.5	$8.9 \pm 0.6 \pm 0.8$	$\frac{1}{2}^-$
$\Xi_c(2790)^0$	2792.8 ± 1.2	$10.0 \pm 0.7 \pm 0.8$	$\frac{1}{2}^-$
$\Xi_c(2815)^+$	2816.67 ± 0.31	$2.43 \pm 0.20 \pm 0.17$	$\frac{3}{2}^-$
$\Xi_c(2815)^0$	2820.22 ± 0.32	$2.54 \pm 0.18 \pm 0.17$	$\frac{3}{2}^-$
$\Xi_c(2930)$	$2931 \pm 3 \pm 5$	$36 \pm 7 \pm 11$	??
$\Xi_c(2970)^+$	2969.4 ± 0.8	$20.9^{+2.4}_{-3.5}$	??
$\Xi_c(2970)^0$	2967.8 ± 0.8	$28.1^{+3.4}_{-4.0}$	??
$\Xi_c(3055)^+$	3055.9 ± 0.4	$7.8 \pm 1.2 \pm 1.5$	??
$\Xi_c(3080)^+$	3077.2 ± 0.4	3.6 ± 1.1	??
$\Xi_c(3080)^0$	3079.9 ± 1.4	5.6 ± 2.2	??
$\Xi_c(3123)^+$	$3122.9 \pm 1.3 \pm 0.3$	$4.4 \pm 3.4 \pm 1.7$	??
Ω_c^0	2695.2 ± 1.7	–	$\frac{1}{2}^+$
$\Omega_c(2770)^0$	2765.9 ± 2.0	–	$\frac{3}{2}^+$
$\Omega_c(3000)^0$	$3000.4 \pm 0.2 \pm 0.1 \pm 0.3$	$4.5 \pm 0.6 \pm 0.3$	??
$\Omega_c(3050)^0$	$3050.2 \pm 0.1 \pm 0.1 \pm 0.3$	< 1.2	??
$\Omega_c(3065)^0$	$3065.6 \pm 0.1 \pm 0.3 \pm 0.3$	$3.5 \pm 0.4 \pm 0.2$	??
$\Omega_c(3090)^0$	$3090.2 \pm 0.3 \pm 0.5 \pm 0.3$	$8.7 \pm 1.0 \pm 0.8$	??
$\Omega_c(3120)^0$	$3119.1 \pm 0.3 \pm 0.9 \pm 0.3$	< 2.1	??

and $\Sigma_c(2520)^{++}K^-$ final states, respectively. These were also seen by the Belle collaboration [13]. Two isodoublet baryonic states of $\Xi_c(2970)$ and $\Xi_c(3080)$ have been measured by BABAR [12] and the Belle [14,15] collaborations. In 2017, the LHCb collaboration [16] observed the five new narrow resonances $\Omega_c(3000)^0$, $\Omega_c(3050)^0$, $\Omega_c(3066)^0$, $\Omega_c(3090)^0$ and $\Omega_c(3119)^0$ decaying into $\Xi_c^+ K^-$. The spin–parity of these excited strange charmed baryons are not confirmed yet, as shown in Table 1. The J^P value assignment of the heavy–light hadrons is very crucial, because they can help to probe their properties as form factors, decay widths, branching fractions, hyperfine splittings, etc. That allows to look back to the theory and the phenomenological study. In Ref. [17], the authors solved light quark cluster–heavy quark picture with the help of the Cornell potential in the framework of nonrelativistic constitute quark model. They calculate the masses of radial excited states $2S$ and $3S$ as well as the orbital excited states $1P$, $2P$ and $1D$ of charmed (Λ_c^+, Σ_c) and charmed-strange (Ξ_c, Ξ_c') baryons by considering an equal up (u) and down (d) quarks masses. So they cannot

distinguish the mass spectra of an isodoublet Ξ_c^0 and Ξ_c^+ (or $\Xi_c'^0$ and $\Xi_c'^+$) baryons. Shah et al. [18,19] used nonrelativistic approach of hypercentral constituent quark model (hCQM) and calculate the excited-state masses of singly charmed baryons. The hyper-Coulomb potential with linear potential of power index ν, varying from 0.5 to 2.0, is used as a long-range spin-independent potential. The mass spectra of isodoublet Ξ_c baryons are calculated separately by considering an unequal u and d quarks masses. Reference [20] solved the three-body bound-state problems using the Gaussian expansion method in the nonrelativistic framework of a constituent quark model. The harmonic oscillator potential is used as a scalar confinement potential. On choosing equal u and d quarks masses, the excited-state mass spectra of Λ_c^+, Σ_c and Ω_c^0 baryons are calculated in the two different excited modes, say λ and ρ. The nonrelativistic Hamiltonian quark model inspired by Isgur and Karl model calculates the masses of baryons containing one, two and three heavy-flavor quarks in Ref. [21] with equal u and d quarks masses. Additionally, they introduced the heavy quark effective theory (HQET) that predicts the degeneracy in baryonic multiplets containing a single heavy quark in terms of quark model quantum numbers. Ebert et al. [22,23] calculated the mass spectra of heavy baryons in the quantum chromodynamics (QCD)-motivated relativistic heavy quark–light diquark model. Reference [24] derived a mass formula analytically for the excited heavy–light hadrons within the framework of relativistic flux tube model, where the heavy quark–light diquark picture is considered. Such formula is applied to determine the masses of Λ_Q and Ξ_Q (Q $=c/b$) baryons. The authors of Ref. [25] obtained the masses of one heavy quark baryons in the heavy quark limit. Chen et al. [26] studied the mass spectra of P wave charmed baryons using the QCD sum rule in the framework of HQET. Reference [27] used the Faddeev method and solved the three-quark problem in momentum space and calculated the masses of singly, doubly and triply heavy baryons. Reference [28] derived some useful mass relations for hadrons using quasilinear Regge trajectory ansatz and make a J^P assignments of $\Xi_c(2980)$, $\Xi_c(3055)$, $\Xi_c(3077)$ and $\Xi_c(3123)$ baryons. Reference [29] determined the ground-state and the first excited-state masses of singly and doubly charmed baryons of spin 1/2 and 3/2 with positive and negative parity. Mathur et al. [30] used quenched lattice nonrelativistic QCD approach and computed the mass spectrum of charmed and bottom baryons.

The strange singly charmed baryons contain one charm quark (c), one strange quark (s) and one light quark (u, d and s) out of these three quarks. This provides an excellent ground for testing the heavy quark symmetry of the heavy quark and the chiral symmetry of the light quarks in a low-energy regime. The strong decay of singly charmed baryons was conveniently studied in the framework of heavy hadron chiral perturbation theory (HHChPT) by which the heavy quark symmetry and the chiral symmetry are incorporated. The chiral Lagrangians corresponding to the strong decay of singly charmed baryons were constructed in Refs. [31–33] for the S, P and D wave transitions. The electromagnetic or weak decays of singly charmed baryons are not well established, and their evidence is not found experimentally yet. Several approaches are used for computing the properties of singly charmed baryons: heavy baryon chiral perturbation theory (HBChPT) [34–36], $SU(3)$ chiral quark soliton model [37], pion mean-field approach [38], chiral structure model [39], covariant chiral perturbation theory [40], large N_c limit [41], chiral quark model [42], nonrelativistic constituent quark model [43–46], lattice QCD [47,48], the bag model [49], light-cone QCD sum rule [50,51], $SU(4)$ chiral constituent quark model (χCQM) [52], relativistic constituent quark model [53,54], light front quark model [55], the $^3P_0$ model [56] and others.

Our effort is to calculate the radial ($2S$–$6S$) and the orbital ($1P$–$5P$, $1D$–$5D$, $1F$–$4F$, $1G$–$3G$ and $1H$–$2H$) excited-state masses of strange singly charmed baryons, for orbital quantum number $L = 0, 1, 2, 3, 4, 5$, in the framework of nonrelativistic hypercentral constituent

quark model (hCQM). The vector Coulomb potential with an additional screening component is used as a scalar confinement potential with the first-order correction to give relativistic effect of order $\mathcal{O}(1/m)$. Such calculated masses are allowed to construct the Regge trajectories in (n_r, M^2) and (J, M^2) planes.

This paper is organized as follows. The hCQM and the potential model are described in brief in Sect. 2. We discuss the mass spectra and construct the Regge trajectories in Sect. 3. The strong one-pion decay rates of the isodoublet $\Xi_c(2645)$, $\Xi_c(2790)$ and $\Xi_c(2815)$ baryons are determined separately by using their masses obtained in the present study and PDG-2018, and the properties like magnetic moments and the radiative decay widths of the ground-state strange charmed baryons are presented in Sect. 4. In Sect. 5, we summarize our present work.

2 Methodology

Usually, the relativistic and the nonrelativistic treatments of quantum mechanics are used to study the spectroscopy of heavy- and light-flavored hadrons. Particularly, when dealing with a three-quark system (baryon), the problem is become more challenging. To describe the relative motion of the constituent quarks inside the baryon the Jacobi coordinates ($\boldsymbol{\rho}$ and $\boldsymbol{\lambda}$) are used, which are given by [57,58]

$$\boldsymbol{\rho} = \frac{(\mathbf{r_1} - \mathbf{r_2})}{\sqrt{2}} \quad \text{and} \quad \boldsymbol{\lambda} = \frac{m_1\mathbf{r_1} + m_2\mathbf{r_2} - (m_1 + m_2)\mathbf{r_3}}{\sqrt{m_1^2 + m_2^2 + (m_1 + m_2)^2}}, \tag{1}$$

where $\mathbf{r}_i$ and m_i ($i = 1, 2, 3$) denote the spatial and the mass coordinate of the ith constitute quark. We use hypercentral constituent quark model (hCQM), which is well established for the study of light-, heavy–light- and heavy-flavored baryons [18,59–62]. In hCQM, the Hamiltonian for a baryonic system is

$$H = \frac{P_x^2}{2m} + V(x), \tag{2}$$

where $x = (\rho, \lambda)$ is the radial hypercentral coordinate of the three-quark system written in a six-dimensional space and the hyperangle $\xi = \arctan\left(\frac{\rho}{\lambda}\right)$. $m = \frac{2m_\rho m_\lambda}{m_\rho + m_\lambda}$ gives the reduced mass of the three quarks [57]. The reduced mass m_ρ and m_λ corresponding to the Jacobi coordinates ρ and λ are

$$m_\rho = \frac{2m_1 m_2}{(m_1 + m_2)} \quad \text{and} \quad m_\lambda = \frac{2m_3(m_1^2 + m_1^2 + m_1 m_2)}{(m_1 + m_2)(m_1 + m_2 + m_3)}. \tag{3}$$

Here, m_1, m_2 and m_3 are the constituent quark masses. The isodoublet of the Ξ_c baryons has a different quark constitution: Ξ_c^0 (dsc), Ξ_c^+ (usc) and for the singlet Ω_c^0 baryon the constituent quarks are s, s and c. To calculate the masses of isodoublet Ξ_c baryons separately, we consider the unequal masses of light quarks (u, d) as: $m_u = 0.338$ GeV, $m_d = 0.35$ GeV and $m_s = 0.5$ GeV, and the charm (c) quark mass $m_c = 1.275$ GeV.

The potential $V(x)$ appearing into Eq. (2) is the nonrelativistic hypercentral potential and is divided into spin-independent $V_{\mathrm{SI}}(x)$ and spin-dependent $V_{\mathrm{SD}}(x)$ part of the potential. We introduce $V_{\mathrm{SI}}(x)$ as

$$V_{\mathrm{SI}}(x) = V_{\mathrm{V}}(x) + V_{\mathrm{S}}(x) + V_{\mathrm{I}}(x). \tag{4}$$

Here, the first-order correction $V_{\mathrm{I}}(x) = -C_F C_A \frac{\alpha_S^2}{4x^2}$ is written in the form of Casimir charges, with $C_F = \frac{2}{3}$ and $C_A = 3$ in the fundamental and adjoint representation, respectively [63].

The vector (Coulomb) potential is

$$V_{\mathrm{V}}(x) = -\frac{2}{3}\frac{\alpha_{\mathrm{s}}}{x}, \tag{5}$$

and it gives the interaction between quarks in a baryonic system. α_{s} is the strong running coupling constant and is

$$\alpha_{\mathrm{s}} = \frac{\alpha_{\mathrm{s}}(\mu_0)}{1 + \left(\frac{33-2n_{\mathrm{f}}}{12\pi}\right)\alpha_{\mathrm{s}}(\mu_0)ln\left(\frac{m_1+m_2+m_3}{\mu_0}\right)}. \tag{6}$$

Here, we take $\alpha_{\mathrm{s}}(\mu_0 = 1\,\mathrm{GeV}) = 0.6$ and $n_{\mathrm{f}} = 3$ gives the number of active quark flavors contributing to quark–gluon loops. We choose a screened potential as a scalar (confining) potential:

$$V_{\mathrm{S}}(x) = a\left(\frac{1-\mathrm{e}^{-\mu x}}{\mu}\right), \tag{7}$$

where $a(\approx 0.1)$ is the string tension and $\mu = 0.04\,\mathrm{GeV}$ is the flavor-independent parameter called screening factor. Using a, $\mu(= 0.04\,\mathrm{GeV})$ and quark masses, we fix the ground-state (1S) mass of these baryons to the known experimental value (PDG) [1]. If the value of $\mu = 0.04\,\mathrm{GeV}$ changes by $\pm 10\%$, the changes in the masses of 2S, 3S, 4S, 5S and 6S states are about 0.30%, 0.53%, 0.75%, 0.93% and 1.1%, respectively. For $x \ll \frac{1}{\mu}$, the screened potential is behaving like a linear potential ax and for $x \gg \frac{1}{\mu}$ it becomes a constant $\frac{a}{\mu}$. The mass spectroscopy resulting from a screened potential is interesting: It predicts smaller masses of the higher excited states with respect to a linear potential. (See results in Ref. [18] for $\nu = 1$ and more detailed studies in Ref. [64].) By taking unequal u and d quarks masses, the mass spectra of Ξ_c^0, Ξ_c^+ and Ω_c^0 baryons are calculated in this work.

Using these parameters, we compute the spin-averaged mass of the strange singly charmed baryons. In order to calculate the masses of nL with different J values, the spin-dependent potential $V_{\mathrm{SD}}(x)$ is employed [65–67]:

$$V_{\mathrm{SD}}(x) = V_{\mathrm{SS}}(x)(\mathbf{S}_\rho \cdot \mathbf{S}_\lambda) + V_{\gamma S}(x)(\mathbf{L} \cdot \mathbf{S}) + V_{\mathrm{T}}(x)\left[S^2 - \frac{3(\mathbf{S}\cdot\mathbf{x})(\mathbf{S}\cdot\mathbf{x})}{x^2}\right]. \tag{8}$$

The spin–spin interaction $V_{\mathrm{SS}}(x)$ gives a hyperfine mass splitting, and the spin–orbit $V_{\gamma S}(x)$ and spin–tensor $V_{\mathrm{T}}(x)$ interaction terms give a fine structure of the given baryonic states. (For details see Ref. [18].)

The six-dimensional hyperradial Schrödinger equation is

$$\left[\frac{1}{2m}\left(-\frac{\mathrm{d}^2}{\mathrm{d}x^2} + \frac{\frac{15}{4} + \gamma(\gamma+4)}{x^2}\right) + V(x)\right]\phi_\gamma(x) = E_{\mathrm{B}}\phi_\gamma(x), \tag{9}$$

which solves numerically using Mathematica notebook [68]. $\phi_\gamma(x)$ is the hypercentral radial function, and E_{B} gives the binding energy of the baryonic states. Our computed mass spectra of strange singly charmed baryons are presented in Tables 2, 3, 4, 5, 6, 7 and 8. We discussed them in the next section.

3 Mass spectra and Regge trajectories

The mass spectrum of strange singly charmed baryons is calculated in the nonrelativistic framework of hypercentral constituent quark model (hCQM). The screened potential is used

Table 2 Predicted masses of the radial excited states of strange singly charmed baryons (in GeV)

Particle	State	J^P	Present	[18]	[22]	[17]	[24]	[23]	[25]	[27]	[20]	[21]	PDG [1]
Ξ_c^0	1S	$\frac{1}{2}^+$	2.471	2.470	2.476	2.470	2.467	2.481	2.466	2.471		2.492	2.47091 ± 0.00025
	2S		2.964	2.940	2.959	2.940	2.959	2.923	2.924	3.137			2.9707 ± 0.0022
	3S		3.358	3.339	3.323	3.265	3.325	3.313	3.183				
	4S		3.720	3.726	3.632		3.629						
	5S		4.064	4.107	3.909								
	6S		4.394		4.166								
	1S	$\frac{3}{2}^+$	2.648	2.610	2.654					2.642		2.650	2.64838 ± 0.00021
	2S		3.080	3.038						3.071		2.984	3.0799 ± 0.0014
	3S		3.424	3.399									
	4S		3.763	3.766									
	5S		4.093	4.136									
	6S		4.415										
Ξ_c^+	1S	$\frac{1}{2}^+$	2.467	2.467									2.46793 ± 0.00018
	2S		2.969	2.956									2.968 ± 0.0026
	3S		3.369	3.370									
	4S		3.738	3.772									
	5S		4.088	4.167									
	6S		4.424										
	1S	$\frac{3}{2}^+$	2.646	2.619									2.64557 ± 0.00026
	2S		3.086	3.061									3.0772 ± 0.0004
	3S		3.436	3.435									
	4S		3.781	3.815									
	5S		4.117	4.198									
	6S		4.445										

Table 2 continued

Particle	State	J^P	Present	[18]	[22]	[17]	[24]	[23]	[25]	[27]	[20]	[21]	PDG [1]
Ω_c^0	1S	$\frac{1}{2}^+$	2.696	2.695	2.698			2.698	2.718	2.699	2.731	2.718	2.6952 ± 0.0017
	2S		3.165	3.164	3.088			3.065	3.152	3.159	3.227	3.152	3.1191 ± 0.0003
	3S		3.540	3.561	3.489				3.275		3.292		
	4S		3.895	3.953	3.814				3.299				
	5S		4.238	4.343	4.102								
	6S		4.569										
	1S	$\frac{3}{2}^+$	2.766	2.745	2.768			2.768	2.766	2.767	2.779	2.776	2.7659 ± 0.002
	2S		3.208	3.197	3.123			3.119	3.190	3.202	3.257	3.190	
	3S		3.564	3.580	3.510				3.280		3.285		
	4S		3.911	3.966	3.830				3.321				
	5S		4.248	4.352	4.114								
	6S		4.577										

Table 3 Predicted masses of the orbital excited states of Ξ_c^0 baryon (P and D waves) (in GeV)

State	J^P	Present	[18]	[22]	[17]	[24]	[23]	[25]	[27]	[26]	[21]	PDG [1]
1P	$\frac{1}{2}^-$	2.828	2.796	2.792	2.793	2.779	2.801	2.773	2.799	2.790	2.763	2.7941 ± 0.0005
	$\frac{3}{2}^-$	2.820	2.781	2.819	2.820	2.814	2.820	2.783		2.830	2.784	2.82026 ± 0.00027
	$\frac{1}{2}^-$	2.832	2.803						2.902		2.859	
	$\frac{3}{2}^-$	2.824	2.788								2.871	
	$\frac{5}{2}^-$	2.814	2.769								2.905	
2P	$\frac{1}{2}^-$	3.191	3.170	3.179	3.140	3.195	3.186		3.004			
	$\frac{3}{2}^-$	3.184	3.154	3.201	3.164	3.204	3.199					
	$\frac{1}{2}^-$	3.195	3.178									
	$\frac{3}{2}^-$	3.188	3.162									
	$\frac{5}{2}^-$	3.177	3.140								2.985	
3P	$\frac{1}{2}^-$	3.541	3.546	3.500		3.521						
	$\frac{3}{2}^-$	3.533	3.527	3.519		3.525						
	$\frac{1}{2}^-$	3.545	3.555									
	$\frac{3}{2}^-$	3.537	3.536									
	$\frac{5}{2}^-$	3.527	3.511									
4P	$\frac{1}{2}^-$	3.879	3.919	3.785								
	$\frac{3}{2}^-$	3.871	3.899	3.804								
	$\frac{1}{2}^-$	3.883	3.929									
	$\frac{3}{2}^-$	3.875	3.909									
	$\frac{5}{2}^-$	3.865	3.882									

Table 3 continued

State	J^P	Present	[18]	[22]	[17]	[24]	[23]	[25]	[27]	[26]	[21]	PDG [1]
5P	$\frac{1}{2}^-$	4.206	4.293	4.048								
	$\frac{3}{2}^-$	4.199	4.272	4.066								
	$\frac{1}{2}^-$	4.210	4.304									
	$\frac{3}{2}^-$	4.203	4.283									
	$\frac{5}{2}^-$	4.193	4.254									
1D	$\frac{3}{2}^+$	3.116	3.080	3.059	3.033	3.055	3.030	3.012				
	$\frac{5}{2}^+$	3.103	3.054	3.076	3.040	3.076	3.042	3.004	3.049		2.995	
	$\frac{1}{2}^+$	3.131	3.108									
	$\frac{3}{2}^+$	3.121	3.089									
	$\frac{5}{2}^+$	3.108	3.064						3.132			
	$\frac{7}{2}^+$	3.092	3.032							3.100		
2D	$\frac{3}{2}^+$	3.464	3.450	3.388		3.407	3.411					
	$\frac{5}{2}^+$	3.452	3.422	3.407		3.416	3.413					
	$\frac{1}{2}^+$	3.478	3.480									
	$\frac{3}{2}^+$	3.469	3.460									
	$\frac{5}{2}^+$	3.457	3.432									
	$\frac{7}{2}^+$	3.442	3.398									

Table 3 continued

State	J^P	Present	[18]	[22]	[17]	[24]	[23]	[25]	[27]	[26]	[21]	PDG [1]
3D	$\frac{3}{2}^+$	3.804		3.678								
	$\frac{5}{2}^+$	3.792		3.699								
	$\frac{1}{2}^+$	3.817										
	$\frac{3}{2}^+$	3.308										
	$\frac{5}{2}^+$	3.796										
	$\frac{7}{2}^+$	3.782										
4D	$\frac{3}{2}^+$	4.132		3.945								
	$\frac{5}{2}^+$	4.121		3.965								
	$\frac{1}{2}^+$	4.144										
	$\frac{3}{2}^+$	4.136										
	$\frac{5}{2}^+$	4.125										
	$\frac{7}{2}^+$	4.112										
5D	$\frac{3}{2}^+$	4.450										
	$\frac{5}{2}^+$	4.442										
	$\frac{1}{2}^+$	4.459										
	$\frac{3}{2}^+$	4.453										
	$\frac{5}{2}^+$	4.445										
	$\frac{7}{2}^+$	4.435										

Table 4 Predicted masses of the orbital excited states of Ξ_c^0 baryon (F, G and H waves) (in GeV)

State	J^P	Present	[18]	[22]	[24]	[23]
1F	$\frac{5}{2}^-$	3.388	3.352	3.278	3.286	3.219
	$\frac{7}{2}^-$	3.369	3.316	3.292	3.302	3.208
	$\frac{3}{2}^-$	3.408	3.392			
	$\frac{5}{2}^-$	3.393	3.363			
	$\frac{7}{2}^-$	3.375	3.327			
	$\frac{9}{2}^-$	3.358	3.283			
2F	$\frac{5}{2}^-$	3.727		3.575		
	$\frac{7}{2}^-$	3.710		3.592		
	$\frac{3}{2}^-$	3.745				
	$\frac{5}{2}^-$	3.732				
	$\frac{7}{2}^-$	3.715				
	$\frac{9}{2}^-$	3.695				
3F	$\frac{5}{2}^-$	4.055		3.845		
	$\frac{7}{2}^-$	4.042		3.865		
	$\frac{3}{2}^-$	4.069				
	$\frac{5}{2}^-$	4.059				
	$\frac{7}{2}^-$	4.046				
	$\frac{9}{2}^-$	4.030				
4F	$\frac{5}{2}^-$	4.376		4.098		
	$\frac{7}{2}^-$	4.364		4.120		
	$\frac{3}{2}^-$	4.388				
	$\frac{5}{2}^-$	4.379				
	$\frac{7}{2}^-$	4.368				
	$\frac{9}{2}^-$	4.354				
1G	$\frac{7}{2}^+$	3.647		3.469		
	$\frac{9}{2}^+$	3.627		3.483		
	$\frac{5}{2}^+$	3.670				
	$\frac{7}{2}^+$	3.653				
	$\frac{9}{2}^+$	3.632				
	$\frac{11}{2}^+$	3.608				
2G	$\frac{7}{2}^+$	3.981		3.745		
	$\frac{9}{2}^+$	3.960		3.763		
	$\frac{5}{2}^+$	4.004				
	$\frac{7}{2}^+$	3.986				
	$\frac{9}{2}^+$	3.965				

Table 4 continued

State	J^P	Present	[18]	[22]	[24]	[23]
	$\frac{11}{2}^+$	3.940				
$3G$	$\frac{7}{2}^+$	4.303				
	$\frac{9}{2}^+$	4.285				
	$\frac{5}{2}^+$	4.323				
	$\frac{7}{2}^+$	4.308				
	$\frac{9}{2}^+$	4.290				
	$\frac{11}{2}^+$	4.268				
$1H$	$\frac{9}{2}^-$	3.905		3.643		
	$\frac{11}{2}^-$	3.877		3.658		
	$\frac{7}{2}^-$	3.936				
	$\frac{9}{2}^-$	3.911				
	$\frac{11}{2}^-$	3.883				
	$\frac{13}{2}^-$	3.850				
$2H$	$\frac{9}{2}^-$	4.229				
	$\frac{11}{2}^-$	4.204				
	$\frac{7}{2}^-$	4.256				
	$\frac{9}{2}^-$	4.234				
	$\frac{11}{2}^-$	4.210				
	$\frac{13}{2}^-$	4.181				

as a scalar potential with the first-order correction. Our calculated masses of the radial excited states (2S–6S) are presented in Table 2 and the orbital excited states (1P–5P, 1D–5D, 1F–4F, 1G–3G and 1H and 2H) are listed in Tables 3, 4, 5, 6, 7 and 8. Our results are compared with other theoretical predictions and the experimental observations where available. The obtained masses are used to draw Regge trajectories in the (n_r, M^2) and (J, M^2) planes. They are used to determine the possible quantum number of the particular hadronic states [28]. The S states with $J^P = \frac{1}{2}^+$ and the P, D, F, G and H states for the J^P values $\frac{1}{2}^-$, $\frac{5}{2}^+$, $\frac{7}{2}^-$, $\frac{9}{2}^+$ and $\frac{11}{2}^-$, respectively, are plotted in the (n_r, M^2) plane. Using the equation,

$$n_r = \beta M^2 + \beta_0, \tag{10}$$

where $n_r = n - 1$ and β and β_0 are the fitted slopes and the intercepts, respectively. In the (J, M^2) plane, the Regge trajectories are plotted with natural $P = (-1)^{J-\frac{1}{2}}$ and the unnatural $P = (-1)^{J+\frac{1}{2}}$ parities. Therefore, the states with J^P values $\frac{1}{2}^+$, $\frac{3}{2}^-$, $\frac{5}{2}^+$, $\frac{7}{2}^-$, $\frac{9}{2}^+$ and $\frac{11}{2}^-$ are here available with the natural parity; and the states $\frac{3}{2}^+$, $\frac{5}{2}^-$, $\frac{7}{2}^+$, $\frac{9}{2}^-$, $\frac{11}{2}^+$ and $\frac{13}{2}^-$ are for the unnatural parity. Using the equation,

$$J = \alpha M^2 + \alpha_0, \tag{11}$$

Table 5 Predicted masses of the orbital excited states of Ξ_c^+ baryon (P and D waves) (in GeV)

State	J^P	Present	[18]	PDG [1]
$1P$	$\frac{1}{2}^-$	2.830	2.810	2.7924 ± 0.0005
	$\frac{3}{2}^-$	2.822	2.794	2.81673 ± 0.00021
	$\frac{1}{2}^-$	2.834	2.818	
	$\frac{3}{2}^-$	2.826	2.802	
	$\frac{5}{2}^-$	2.815	2.780	
$2P$	$\frac{1}{2}^-$	3.200	3.198	
	$\frac{3}{2}^-$	3.192	3.180	
	$\frac{1}{2}^-$	3.204	3.208	
	$\frac{3}{2}^-$	3.196	3.189	
	$\frac{5}{2}^-$	3.185	3.165	
$3P$	$\frac{1}{2}^-$	3.556	3.586	
	$\frac{3}{2}^-$	3.547	3.566	
	$\frac{1}{2}^-$	3.560	3.596	
	$\frac{3}{2}^-$	3.551	3.576	
	$\frac{5}{2}^-$	3.540	3.549	
$4P$	$\frac{1}{2}^-$	3.899	3.974	
	$\frac{3}{2}^-$	3.891	3.952	
	$\frac{1}{2}^-$	3.903	3.985	
	$\frac{3}{2}^-$	3.895	3.963	
	$\frac{5}{2}^-$	3.885	3.933	
$5P$	$\frac{1}{2}^-$	4.233	4.360	
	$\frac{3}{2}^-$	4.225	4.338	
	$\frac{1}{2}^-$	4.237	4.372	
	$\frac{3}{2}^-$	4.229	4.349	
	$\frac{5}{2}^-$	4.219	4.319	
$1D$	$\frac{3}{2}^+$	3.123	3.104	3.1229 ± 0.0013
	$\frac{5}{2}^+$	3.109	3.077	
	$\frac{1}{2}^+$	3.138	3.134	
	$\frac{3}{2}^+$	3.128	3.114	
	$\frac{5}{2}^+$	3.114	3.087	
	$\frac{7}{2}^+$	3.097	3.053	
$2D$	$\frac{3}{2}^+$	3.478	3.485	
	$\frac{5}{2}^+$	3.465	3.458	
	$\frac{1}{2}^+$	3.493	3.516	
	$\frac{3}{2}^+$	3.483	3.495	

Table 5 continued

State	J^P	Present	[18]	PDG [1]
	$\frac{5}{2}^+$	3.470	3.468	
	$\frac{7}{2}^+$	3.453	3.434	
3D	$\frac{3}{2}^+$	3.823		
	$\frac{5}{2}^+$	3.810		
	$\frac{1}{2}^+$	3.836		
	$\frac{3}{2}^+$	3.827		
	$\frac{5}{2}^+$	3.815		
	$\frac{7}{2}^+$	3.800		
4D	$\frac{3}{2}^+$	4.157		
	$\frac{5}{2}^+$	4.146		
	$\frac{1}{2}^+$	4.170		
	$\frac{3}{2}^+$	4.162		
	$\frac{5}{2}^+$	4.150		
	$\frac{7}{2}^+$	4.136		
5D	$\frac{3}{2}^+$	4.483		
	$\frac{5}{2}^+$	4.472		
	$\frac{1}{2}^+$	4.494		
	$\frac{3}{2}^+$	4.487		
	$\frac{5}{2}^+$	4.476		
	$\frac{7}{2}^+$	4.463		

where α and α_0 are the fitted slopes and the intercepts, respectively. The Regge trajectories of the strange singly charmed baryons are shown in Figs. 1, 2, 3, 4, 5 and 6 plotted in the (n_r, M^2) and (J, M^2) planes using the above equations. On the Regge lines, our calculated masses are presented and the available experimental observations are indicated by a cross sign with a possible quantum number.

3.1 Ξ_c states

The spin–parity of the ground (1S) state of Ξ_c^+ baryon and its neutral isospin partner Ξ_c^0 were confirmed experimentally. For the predictions of the excited radial and orbital states of isodoublet Ξ_c baryons, we fixed their masses of Ξ_c^+ : 2.46787 ± 0.0003 GeV and Ξ_c^0 : $2.47087^{+0.00028}_{-0.00031}$ GeV for $J^P = \frac{1}{2}^+$; and for the $J^P = \frac{3}{2}^+$ the Ξ_c^+ : 2.64553 ± 0.00031 GeV and Ξ_c^0 : 2.64632 ± 0.00031 GeV from [1]. The isodoublet of Ξ_c baryons [$\Xi_c^0(dsc)$ and $\Xi_c^+(usc)$] has different quark constituents. The authors of Refs. [17,21–25,27] consider equal mass of light quarks u and d. So they cannot distinguish the isodoublet of Ξ_c baryons and calculate their excited-state masses. In this work, we use $m_u = 0.338$ GeV and $m_d = 0.350$ GeV taken from Ref. [18] and we calculate the mass spectra of $\Xi_c^0(dsc)$ and $\Xi_c^+(usc)$ baryons separately (see Tables 2, 3, 4, 5 and 6). So we can compare our results with the

Table 6 Predicted masses of the orbital excited states of Ξ_c^+ baryon (F, G and H waves) (in GeV)

State	J^P	Present	[18]
1F	$\frac{5}{2}^-$	3.380	3.394
	$\frac{7}{2}^-$	3.357	3.354
	$\frac{3}{2}^-$	3.420	3.432
	$\frac{5}{2}^-$	3.405	3.406
	$\frac{7}{2}^-$	3.386	3.366
	$\frac{9}{2}^-$	3.363	3.318
2F	$\frac{5}{2}^-$	3.744	
	$\frac{7}{2}^-$	3.727	
	$\frac{3}{2}^-$	3.762	
	$\frac{5}{2}^-$	3.749	
	$\frac{7}{2}^-$	3.732	
	$\frac{9}{2}^-$	3.712	
3F	$\frac{5}{2}^-$	4.079	
	$\frac{7}{2}^-$	4.065	
	$\frac{3}{2}^-$	4.094	
	$\frac{5}{2}^-$	4.083	
	$\frac{7}{2}^-$	4.069	
	$\frac{9}{2}^-$	4.052	
4F	$\frac{5}{2}^-$	4.407	
	$\frac{7}{2}^-$	4.393	
	$\frac{3}{2}^-$	4.422	
	$\frac{5}{2}^-$	4.411	
	$\frac{7}{2}^-$	4.397	
	$\frac{9}{2}^-$	4.381	
1G	$\frac{7}{2}^+$	3.667	
	$\frac{9}{2}^+$	3.642	
	$\frac{5}{2}^+$	3.694	
	$\frac{7}{2}^+$	3.673	
	$\frac{9}{2}^+$	3.648	
	$\frac{11}{2}^+$	3.619	
2G	$\frac{7}{2}^+$	4.002	
	$\frac{9}{2}^+$	3.981	
	$\frac{5}{2}^+$	4.024	
	$\frac{7}{2}^+$	4.007	
	$\frac{9}{2}^+$	3.987	

Table 6 continued	State	J^P	Present	[18]
		$\frac{11}{2}^+$	3.963	
	$3G$	$\frac{7}{2}^+$	4.332	
		$\frac{9}{2}^+$	4.312	
		$\frac{5}{2}^+$	4.353	
		$\frac{7}{2}^+$	4.337	
		$\frac{9}{2}^+$	4.317	
		$\frac{11}{2}^+$	4.294	
	$1H$	$\frac{9}{2}^-$	3.926	
		$\frac{11}{2}^-$	3.896	
		$\frac{7}{2}^-$	3.958	
		$\frac{9}{2}^-$	3.932	
		$\frac{11}{2}^-$	3.903	
		$\frac{13}{2}^-$	3.869	
	$2H$	$\frac{9}{2}^-$	4.255	
		$\frac{11}{2}^-$	4.230	
		$\frac{7}{2}^-$	4.281	
		$\frac{9}{2}^-$	4.260	
		$\frac{11}{2}^-$	4.236	
		$\frac{13}{2}^-$	4.208	

predictions of Refs. [17,21–25,27] with either $\varXi_c^0$ baryon or either $\varXi_c^+$ baryon. In this work, our results of radial and orbital excited states of $\varXi_c^0$ baryon are compared with the predictions of Refs. [17,21–25,27].

In 2016, the Belle collaboration [69] studied the decay of an isodoublet of $\varXi_c(2790)$ and $\varXi_c(2815)$ into $\varXi_c^0$ and $\varXi_c^+$ final states. They identified $\varXi_c(2790)$ and $\varXi_c(2815)$ states with the total spin $\frac{1}{2}^-$ and $\frac{3}{2}^-$, respectively. According to the quark mass hierarchy, the down (d) quark is heavier than up (u) quark. So the $\varXi_c^0$ are expected to be heavier than $\varXi_c^+$ masses. Reference [69] gives a negative isospin mass splittings of the $\varXi_c$ isodoublets; $M(\varXi_c(2645)^+ - \varXi_c(2645)^0)$, $M(\varXi_c(2790)^+ - \varXi_c(2790)^0)$, $M(\varXi_c(2815)^+ - \varXi_c(2815)^0)$, $M(\varXi_c(2970)^+ - \varXi_c(2970)^0)$ and $M(\varXi_c(3080)^+ - \varXi_c(3080)^0)$. In the present study, the isospin mass splittings are positive, i.e., $\varXi_c^+ > \varXi_c^0$. (See Ref. [70] to know about isospin mass splitting.)

Also, Ref. [69] observed an isodoublet $\varXi_c(2970)$ resonances, but still their J^P values are not found. Their world average masses are 2.9707 ± 0.0022 GeV and 2.968 ± 0.0026 GeV [1]. These are in accordance with our predictions of $2S$ state with $J^P = \frac{1}{2}^+$. The world average masses of the isodoublet of $\varXi_c(3080)$ are 3.0772 ± 0.0004 GeV and 3.0799 ± 0.0014 GeV [1], which are in agreement with our predictions of a $2S$ state with $J^P = \frac{3}{2}^+$ (see Table 2). The BABAR collaboration [12] reported a state $\varXi_c(3123)^+$ of mass $3.1229 \pm 0.0013\text{(stat)} \pm 0.0003\text{(syst)}$ GeV. This is exactly matched by our prediction of the second orbital excitation of $\varXi_c^+$ with $J^P = \frac{3}{2}^+$; for the spin $S = \frac{1}{2}$ (see Tables 5 and 6).

Table 7 Predicted masses of the orbital excited states of Ω_c^0 baryon (P and D waves) (in GeV)

State	J^P	Present	[18]	[22]	[23]	[25]	[27]	[20]	[26]	[21]	PDG [1]
1P	$\frac{1}{2}^-$	2.976	3.041	3.055	3.025	3.046	3.035	3.030	3.250	2.977	3.0004 ± 0.00021
	$\frac{3}{2}^-$	2.968	3.024	3.054	3.026	3.056	3.125	3.033	3.260	2.986	
	$\frac{1}{2}^-$	2.979	3.050	2.966	3.020			3.048		2.970	
	$\frac{3}{2}^-$	2.972	3.033	3.029	2.998	2.986		3.056	3.270	2.994	
	$\frac{5}{2}^-$	2.962	3.010	3.051	3.022	3.014		3.057	3.320	3.014	
2P	$\frac{1}{2}^-$	3.341	3.427	3.435	3.376						
	$\frac{3}{2}^-$	3.334	3.408	3.433	3.374						
	$\frac{1}{2}^-$	3.345	3.436	3.384	3.371						
	$\frac{3}{2}^-$	3.337	3.417	3.415	3.350						
	$\frac{5}{2}^-$	3.328	3.393	3.427	3.365						
3P	$\frac{1}{2}^-$	3.694	3.813	3.754							
	$\frac{3}{2}^-$	3.687	3.793	3.752							
	$\frac{1}{2}^-$	3.699	3.823	3.717							
	$\frac{3}{2}^-$	3.690	3.803	3.737							
	$\frac{5}{2}^-$	3.681	3.777	3.744							
4P	$\frac{1}{2}^-$	4.036	4.199	4.037							
	$\frac{3}{2}^-$	4.029	4.179	4.036							
	$\frac{1}{2}^-$	4.040	4.209	4.009							
	$\frac{3}{2}^-$	4.033	4.189	4.023							
	$\frac{5}{2}^-$	4.023	4.162	4.028							

Table 7 continued

State	J^P	Present	[18]	[22]	[23]	[25]	[27]	[20]	[26]	[21]	PDG [1]
5P	$\frac{1}{2}^-$	4.369	4.587								
	$\frac{3}{2}^-$	4.362	4.565								
	$\frac{1}{2}^-$	4.373	4.598								
	$\frac{3}{2}^-$	4.366	4.576								
	$\frac{5}{2}^-$	4.356	4.547								
1D	$\frac{3}{2}^+$	3.264	3.325	3.298	3.215	3.262					
	$\frac{5}{2}^+$	3.251	3.299	3.297	3.218	3.273				3.196	
	$\frac{1}{2}^+$	3.277	3.354	3.287	3.222						
	$\frac{3}{2}^+$	3.268	3.335	3.282	3.217						
	$\frac{5}{2}^+$	3.256	3.308	3.286	3.187					3.203	
	$\frac{7}{2}^+$	3.241	3.276	3.283	3.237					3.206	
2D	$\frac{3}{2}^+$	3.616	3.709	3.627							
	$\frac{5}{2}^+$	3.604	3.680	3.626							
	$\frac{1}{2}^+$	3.629	3.741	3.623							
	$\frac{3}{2}^+$	3.620	3.719	3.613							
	$\frac{5}{2}^+$	3.608	3.691	3.614							
	$\frac{7}{2}^+$	3.594	3.656	3.611							
3D	$\frac{3}{2}^+$	3.958									
	$\frac{5}{2}^+$	3.947									
	$\frac{1}{2}^+$	3.971									

Table 7 continued

State	J^P	Present	[18]	[22]	[23]	[25]	[27]	[20]	[26]	[21]	PDG [1]
	$\frac{3}{2}^+$	3.962									
	$\frac{5}{2}^+$	3.951									
	$\frac{7}{2}^+$	3.938									
4D	$\frac{3}{2}^+$	4.292									
	$\frac{5}{2}^+$	4.282									
	$\frac{1}{2}^+$	4.303									
	$\frac{3}{2}^+$	4.296									
	$\frac{5}{2}^+$	4.285									
	$\frac{7}{2}^+$	4.273									
5D	$\frac{3}{2}^+$	4.617									
	$\frac{5}{2}^+$	4.608									
	$\frac{1}{2}^+$	4.628									
	$\frac{3}{2}^+$	4.621									
	$\frac{5}{2}^+$	4.611									
	$\frac{7}{2}^+$	4.599									

Table 8 Predicted masses of the orbital excited states of Ω_c^0 baryon (F, G and H waves) (in GeV)

State	J^P	Present	[18]	[22]
$1F$	$\frac{5}{2}^-$	3.536	3.602	3.522
	$\frac{7}{2}^-$	3.519	3.565	3.498
	$\frac{3}{2}^-$	3.555	3.643	3.533
	$\frac{5}{2}^-$	3.541	3.613	3.515
	$\frac{7}{2}^-$	3.524	3.577	3.514
	$\frac{9}{2}^-$	3.503	3.532	3.485
$2F$	$\frac{5}{2}^-$	3.878		
	$\frac{7}{2}^-$	3.863		
	$\frac{3}{2}^-$	3.895		
	$\frac{5}{2}^-$	3.883		
	$\frac{7}{2}^-$	3.868		
	$\frac{9}{2}^-$	3.850		
$3F$	$\frac{5}{2}^-$	4.213		
	$\frac{7}{2}^-$	4.199		
	$\frac{3}{2}^-$	4.229		
	$\frac{5}{2}^-$	4.218		
	$\frac{7}{2}^-$	4.204		
	$\frac{9}{2}^-$	4.186		
$4F$	$\frac{5}{2}^-$	4.541		
	$\frac{7}{2}^-$	4.527		
	$\frac{3}{2}^-$	4.556		
	$\frac{5}{2}^-$	4.545		
	$\frac{7}{2}^-$	4.531		
	$\frac{9}{2}^-$	4.515		
$1G$	$\frac{7}{2}^+$	3.800		3.721
	$\frac{9}{2}^+$	3.777		3.685
	$\frac{5}{2}^+$	3.824		3.739
	$\frac{7}{2}^+$	3.806		3.707
	$\frac{9}{2}^+$	3.783		3.705
	$\frac{11}{2}^+$	3.756		3.665
$2G$	$\frac{7}{2}^+$	4.136		
	$\frac{9}{2}^+$	4.115		
	$\frac{5}{2}^+$	4.158		

Table 8 continued

State	J^P	Present	[18]	[22]
	$\frac{7}{2}^+$	4.141		
	$\frac{9}{2}^+$	4.120		
	$\frac{11}{2}^+$	4.096		
$3G$	$\frac{7}{2}^+$	4.461		
	$\frac{9}{2}^+$	4.445		
	$\frac{5}{2}^+$	4.478		
	$\frac{7}{2}^+$	4.465		
	$\frac{9}{2}^+$	4.449		
	$\frac{11}{2}^+$	4.431		
$1H$	$\frac{9}{2}^-$	4.057		
	$\frac{11}{2}^-$	4.029		
	$\frac{7}{2}^-$	4.087		
	$\frac{9}{2}^-$	4.063		
	$\frac{11}{2}^-$	4.035		
	$\frac{13}{2}^-$	4.004		
$2H$	$\frac{9}{2}^-$	4.386		
	$\frac{11}{2}^-$	4.362		
	$\frac{7}{2}^-$	4.412		
	$\frac{9}{2}^-$	4.391		
	$\frac{11}{2}^-$	4.367		
	$\frac{13}{2}^-$	4.339		

For the radial excitation of Ξ_c^0 baryon, with $J^P = \frac{1}{2}^+$ and $J^P = \frac{3}{2}^+$, our predictions are larger than Refs. [17,22,23,25,27]. For the P and D states, our results are in accordance with the predictions of Refs. [17,22–24]. And for $1F$ to $4F$, $1G$–$2G$ and $1H$ states our predictions are larger than Ref. [22] by mass differences between 77 MeV and 262 MeV (see Tables 3, 4). For the isodoublet Ξ_c baryons, our results are in accordance with the predictions of Shah et al. [18]. The other theoretical and phenomenological studies consider the same light quark masses, so here our predictions are compared only with Ξ_c^0 baryon. Our calculated masses of the radial excited states of Ξ_c^+ baryon are presented in Table 2, and their orbital excited states are listed in Tables 5 and 6.

The Regge trajectories of the isodoublet Ξ_c baryons are shown in Figs. 1, 2, 3 and 4. In both the planes (n_r, M^2) and (J, M^2), their squared masses are fit nicely on Regge lines. Regge trajectories confirmed the isodoublet states of $\Xi_c(2790)$ and $\Xi_c(2815)$ as first orbital excited states with spin–parity $\frac{1}{2}^-$ and $\frac{3}{2}^-$, respectively. They predict an isodoublet of $\Xi_c(2970)$ and $\Xi_c(3080)$ as $2S$ states with spin–parity $\frac{1}{2}^+$ and $\frac{3}{2}^+$, respectively. In the present study, the Regge trajectories are enabled for the predictions of the experimental observed states $\Xi_c(2930)$ and $\Xi_c(3055)^+$.
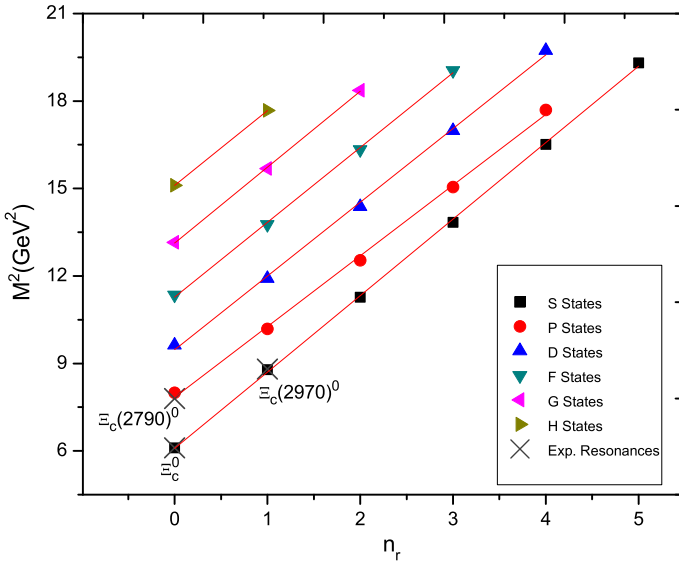
Fig. 1 The ($M^2 \to n_r$) Regge trajectory of Ξ_c^0 baryon
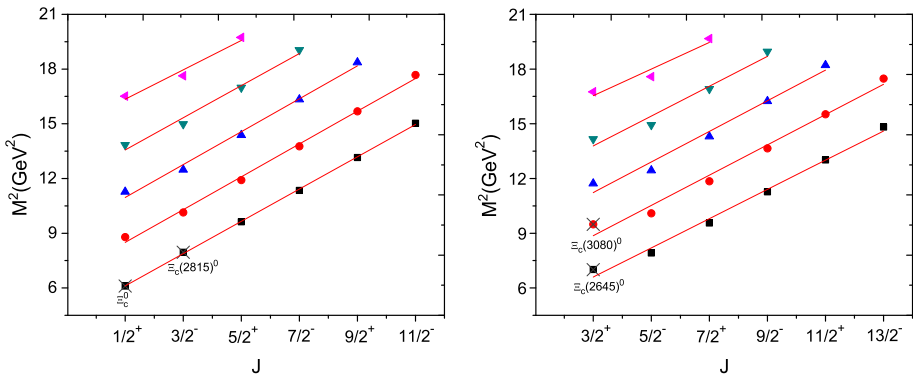
Fig. 2 The ($M^2 \to J$) Regge trajectories of Ξ_c^0 baryon with the natural parity (left) and the unnatural parity (right)

3.2 Ω_c^0 states

Experimentally, only the ground states of Ω_c^0 baryon have been observed with their quantum number. PDG [1] fitted their masses: 2.6952 ± 0.0017 GeV for $J^P = \frac{1}{2}^+$ and 2.7659 ± 0.002 GeV for $J^P = \frac{3}{2}^+$. The $\Omega_c(2770)^0$ was observed by BABAR collaboration [71] in the decay of $\Omega_c(2770)^0 \to \Omega_c^0 + \gamma$. Recently, the LHCb collaboration [16] observed a number of excited states of Ω_c^0 baryon: $\Omega_c(3000)^0$, $\Omega_c(3050)^0$, $\Omega_c(3066)^0$, $\Omega_c(3090)^0$ and $\Omega_c(3119)^0$. Their J^P values are not confirmed yet.

We calculate the masses of radial and orbital excited states of Ω_c^0 baryon. For that, first we fit their ground-state masses from Ref. [1]. The LHCb [16] and the Belle collaboration [72] reported a state $\Omega_c(3000)^0$. The PDG [1] confirmed its world average mass, $3.00041 \pm$
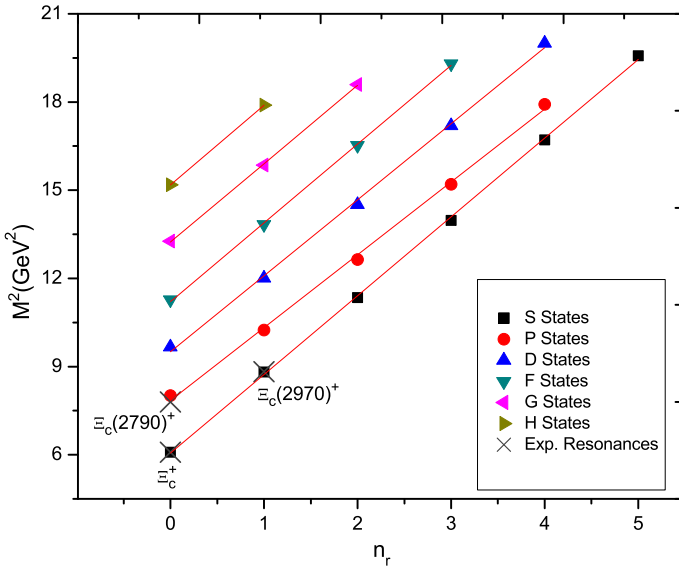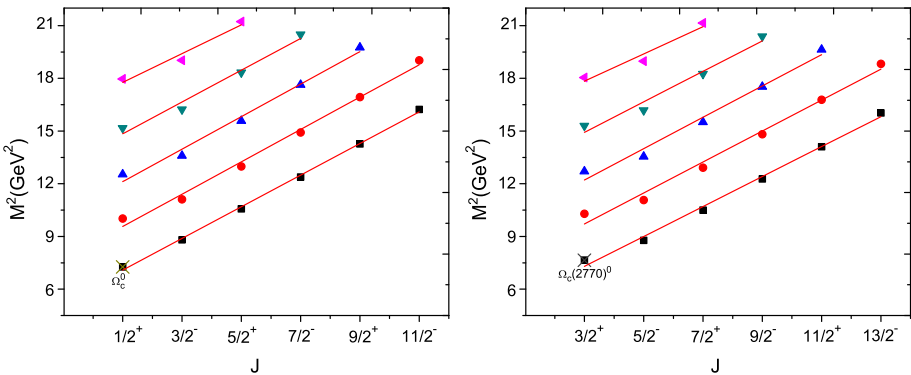
Fig. 3 The $(M^2 \to n_r)$ Regge trajectory of Ξ_c^+ baryon
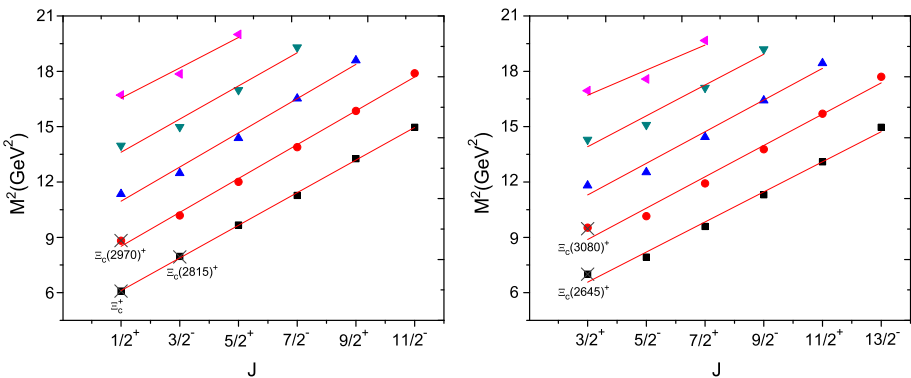
Fig. 4 The $(M^2 \to J)$ Regge trajectories of Ξ_c^+ baryon with the natural parity (left) and the unnatural parity (right)

0.00022 GeV. This state is close to our prediction 2.976 GeV of $1P$ state of $J^P = \frac{1}{2}^-$ with spin $S = \frac{1}{2}$ (see Tables 7 and 8). Also, they report a state $\Omega_c(3119)^0$ measured with the mass $3.1191 \pm 0.0003(\text{stat}) \pm 0.0009^{+0.0003}_{-0.0005}(\text{syst})$ GeV [16]. Such a state might be $2S$ state with $J^P = \frac{1}{2}^+$ (see Table 2). For the radial excited states of Ω_c^0 baryon, with $J^P = \frac{1}{2}^+$ and $J^P = \frac{3}{2}^+$, our results are in agreement with the predictions of Refs. [21,22]. And, for the orbital excitations of $1P$ to $4P$, $1D$–$2D$, $1F$ and $1G$ states, our results are in accordance with the predictions of Refs. [20–23,25–27]. In the Ω_c^0 baryon mass spectrum, the screening effect contributes to predictions of lower masses of the excited radial and orbital states with respect to the results obtained by Shah et al. [18] using the linear potential.

The Regge trajectories of the Ω_c^0 baryon are shown in Figs. 5 and 6. In both the planes (n_r, M^2) and (J, M^2), the squared masses of their excited states are fit nicely on Regge lines.
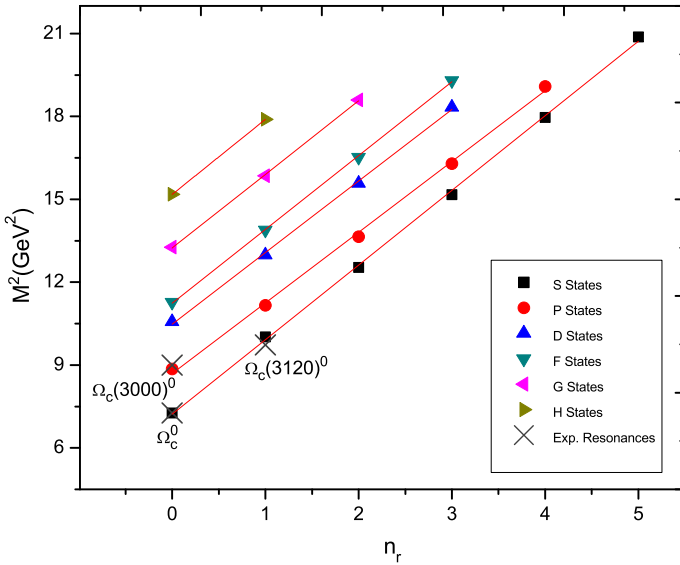
Fig. 5 The ($M^2 \to n_r$) Regge trajectory of Ω_c^0 baryon

Fig. 6 The ($M^2 \to J$) Regge trajectories of Ω_c^0 baryon with the natural parity (left) and the unnatural parity (right)

The $\Omega_c(3000)^0$ is predicted as a first orbital excited state with $J^P = \frac{1}{2}^-$, and the $\Omega_c(3119)^0$ may have $2S$ state with $J^P = \frac{1}{2}^+$. In the present study, the Regge trajectories are enabled for the predictions of the experimental observed states $\Omega_c(3050)^0$, $\Omega_c(3066)^0$ and $\Omega_c(3090)^0$.

4 Properties

4.1 Strong decays

The study of heavy–light-flavored baryons provides an excellent base to update the understanding of heavy quark symmetry of the heavy quark and the SU(3) chiral symmetry of the light quark. As we stated in Introduction, the heavy hadron chiral perturbation theory

(HHChPT) describes a chiral Lagrangian in which both the symmetries are incorporated. Such a Lagrangian derived an expression of the partial decay rates (see Refs. [31–33]) containing strong couplings: g_1 and g_2 for the P wave transitions and h_2 to h_7 for the S wave transitions. And, the pion decay constant $f_\pi = 130.2$ MeV is taken from PDG-2018 [1].

The strong decays of $\Xi_c(2645)^+$ and $\Xi_c(2645)^0$ are governed by the coupling g_2. In our previous work [73], we extract g_2 from the decays: $\Sigma_c(2455)^{++} \to \Lambda_c^+\pi^+$, $\Sigma_c(2455)^0 \to \Lambda_c^+\pi^-$, $\Sigma_c(2520)^{++} \to \Lambda_c^+\pi^+$ and $\Sigma_c(2520)^0 \to \Lambda_c^+\pi^-$ as

$$| g_2 |= 0.550^{+0.013}_{-0.027}, \qquad 0.544^{+0.010}_{-0.018}, \qquad 0.561^{+0.005}_{-0.007}, \qquad 0.570^{+0.007}_{-0.009}, \qquad (12)$$

respectively. Here, we used their masses and respective decay widths from PDG-2018 [1], which are close to $| g_2 |_{2015} = 0.565^{+0.011}_{-0.024}$ and $| g_2 |_{2006} = 0.605^{+0.039}_{-0.043}$ and in accordance with the recent prediction $0.688^{+0.013}_{-0.035}$ of Ref. [39]. The coupling h_2 controls the decay of first orbital excitation of isodoublet Ξ_c baryon. The CDF collaboration [74] studied $\Lambda_c(2595)^+$ resonance into $\Lambda_c^+\pi^+\pi^-$ final state and measured the strong coupling $h_2 = 0.60 \pm 0.07$.

Expression of the strong decay rates of an isodoublet of $\Xi_c(2645)$, $\Xi_c(2790)$ and $\Xi_c(2815)$ is taken from Refs. [31–33]. The masses of these states obtained in the present study and from the PDG-2018 [1] are used to calculate their strong decay rates separately. They are listed into the third and the fourth column of Table 9. Here, in both the cases of masses we employed the same couplings $| g_2 |= 0.550^{+0.013}_{-0.027}$ and $h_2 = 0.60 \pm 0.07$. Our results HHChPT(2019) with PDG-2018[1] update the strong decay rates of these baryonic states. Our calculated decay widths of isodoublet $\Xi_c(2645)$ are in agreement with HHChPT(2015) [4], HHChPT(2007) [32] and the recent observations of Belle collaboration [69]. The decay widths of isodoublet states of $\Xi_c(2790)$ are smaller, and for an isodoublet $\Xi_c(2815)$ our results are larger with respect to Refs. [4,32,69]. Such differences are because of the selection of couplings Ref. [32] used $| g_2 |= 0.605^{+0.039}_{-0.043}$ and $h_2 = 0.437^{+0.114}_{-0.102}$ and Ref. [4] used $| g_2 |= 0.565^{+0.011}_{-0.024}$ and $h_2 = 0.63 \pm 0.07$.

4.2 Magnetic moments

To improve our understanding of the inner structure and geometrical shape of the hadrons, the study of electromagnetic properties is an essential key. The magnetic moment of the hadron is precisely a function of its structure and of its parameters such as spin, flavor, charge and the effective masses of the bound quarks. Its expression can be written in the form of expectation value as [43,44]

$$\mu_B = \sum_q \langle \Phi_{\text{sf}} | \hat{\mu}_{qz} | \Phi_{\text{sf}} \rangle; \qquad q = u, d, s, c. \qquad (13)$$

Here, μ_B and Φ_{sf} denote the magnetic moment and the spin–flavor wave function of the participating baryon. The $\hat{\mu}_{q_z}$ is the z-component of the magnetic moment operator of the individual quark given by

$$\hat{\mu}_{qz} = \frac{e_q}{2m_q^{\text{eff}}} \cdot \sigma_{qz}, \qquad (14)$$

where e_q is the charge and σ_{q_z} is the z-component of the constituent quark spin. The m_q^{eff} is the effective quark mass and is

$$m_q^{\text{eff}} = m_q \left(1 + \frac{\langle H \rangle}{\sum_q m_q} \right). \qquad (15)$$

Table 9 The strong decay widths (in MeV) of Ξ_c baryons

State	Decay Mode	HHChPT Present	HHChPT(2019) PDG-2018	[4]	[32]	[37]	[54]	[55]	[46]	Exp. [69]
$\Xi_c(2645)^+$	$\Xi_c^+\pi^0$	$0.97^{+0.05}_{-0.09}$	$0.92^{+0.04}_{-0.09}$							
	$\Xi_c^0\pi^+$	$1.41^{+0.07}_{-0.13}$	$1.39^{+0.07}_{-0.13}$							
	Total	$2.38^{+0.11}_{-0.23}$	$2.31^{+0.11}_{-0.22}$	2.8 ± 0.4	2.7 ± 0.2		3.04 ± 0.37	1.76 ± 0.14	3.18 ± 0.10	2.06 ± 0.13 ± 0.13
$\Xi_c(2645)^0$	$\Xi_c^+\pi^-$	$1.82^{+0.09}_{-0.17}$	$1.64^{+0.08}_{-0.16}$							
	$\Xi_c^0\pi^0$	$0.90^{+0.04}_{-0.09}$	$0.84^{+0.04}_{-0.08}$							
	Total	$2.72^{+0.13}_{-0.26}$	$2.48^{+0.12}_{-0.24}$	2.9 ± 0.4	2.8 ± 0.2	2.53	3.12 ± 0.33	1.83 ± 0.06	3.03 ± 0.10	2.35 ± 0.18 ± 0.13
$\Xi_c(2790)^+$	$\Xi_c'^+\pi^0$	–	$2.28^{+0.55}_{-0.49}$							
	$\Xi_c'^0\pi^+$	–	$4.71^{+1.16}_{-1.04}$							
	Total	–	$6.99^{+1.71}_{-1.53}$	$8.0^{+4.7}_{-3.3}$	$8.0^{+4.7}_{-3.3}$					8.9 ± 0.6 ± 0.8

Table 9 continued

State	Decay Mode	HHChPT Present	HHChPT(2019) PDG-2018	[4]	[32]	[37]	[54]	[55]	[46]	Exp. [69]
$\Xi_c(2790)^0$	$\Xi_c'^+\pi^-$	—	$4.79^{+1.18}_{-1.05}$							
	$\Xi_c'^0\pi^0$	—	$2.27^{+0.58}_{-0.51}$							
	Total	—	$7.06^{+1.76}_{-1.56}$	$8.5^{+5.0}_{-3.5}$	$8.5^{+5.0}_{-3.5}$					10.0 ± 0.7 ± 0.8
$\Xi_c(2815)^+$	$\Xi_c(2645)^+\pi^0$	$1.58^{+0.39}_{-0.35}$	$1.48^{+0.36}_{-0.32}$							
	$\Xi_c(2645)^0\pi^+$	$3.11^{+0.77}_{-0.68}$	$2.93^{+0.72}_{-0.64}$							
	Total	$4.69^{+1.16}_{-1.03}$	$4.40^{+1.09}_{-0.97}$	$3.4^{+2.0}_{-1.4}$	$3.4^{+2.0}_{-1.4}$		0.70 ± 0.04	2.35 ± 0.93		2.43 ± 0.20 ± 0.17
$\Xi_c(2815)^0$	$\Xi_c(2645)^+\pi^0$	$1.56^{+0.38}_{-0.34}$	$1.57^{+0.39}_{-0.34}$							
	$\Xi_c(2645)^0\pi^+$	$2.99^{+0.76}_{-0.68}$	$3.07^{+0.76}_{-0.68}$							
	Total	$4.54^{+1.12}_{-1.00}$	$4.64^{+1.15}_{-1.02}$	$3.6^{+2.1}_{-1.5}$	$3.6^{+2.1}_{-1.5}$					2.54 ± 0.18 ± 0.17

Reference [4] → HHChPT(2015) PDG-2014 and
Reference [32] → HHChPT(2007) PDG-2006

Equation 15 gives the mass of the bound quark inside the baryons by taking into account its binding interactions with other two quarks. The Hamiltonian $\langle H \rangle$ is obtained by taking the mass difference of the measured or predicted baryon mass M with the sum of the masses of the three constituent quarks $\sum_q m_q$ of the participating baryon, i.e., $\langle H \rangle = M - \sum_q m_q$.

For example, in order to determine the magnetic moment of Ω_c^0 baryon we write Eq. 13 as

$$\mu_{\Omega_c^0} = \left\langle \Phi_{\text{sf}_{\Omega_c^0}} \middle| \hat{\mu}_{qz} \middle| \Phi_{\text{sf}_{\Omega_c^0}} \right\rangle. \tag{16}$$

Here, the spin–flavor wave function (Φ_{sf}) of Ω_c^0 baryon is obtained by taking a combination of flavor and spin part wave function as

$$\left| \Phi_{\text{sf}_{\Omega_c^0}} \right\rangle = \frac{1}{\sqrt{6}} (s \uparrow s \downarrow c \uparrow + s \downarrow s \uparrow c \uparrow - 2s \uparrow s \uparrow c \uparrow). \tag{17}$$

Therefore, Eq. 16 will be

$$\mu_{\Omega_c^0} = \frac{1}{6} \langle s \uparrow s \downarrow c \uparrow + s \downarrow s \uparrow c \uparrow - 2s \uparrow s \uparrow c \uparrow | \hat{\mu}_{qz} | s \uparrow s \downarrow c \uparrow$$
$$+ s \downarrow s \uparrow c \uparrow - 2s \uparrow s \uparrow c \uparrow \rangle. \tag{18}$$

Following the orthogonality of quark flavor and spin states, for example $\langle s \uparrow s \downarrow c \uparrow | s \uparrow s \uparrow c \downarrow \rangle = 0$, the expression for the Ω_c^0 magnetic moment reduces to

$$\mu_{\Omega_c^0} = \frac{1}{6} \langle s \uparrow s \downarrow c \uparrow | \hat{\mu}_{qz} | s \uparrow s \downarrow c \uparrow \rangle$$
$$+ \frac{1}{6} \langle s \downarrow s \uparrow c \uparrow | \hat{\mu}_{qz} | s \downarrow s \uparrow c \uparrow \rangle$$
$$+ \frac{4}{6} \langle s \uparrow s \uparrow c \downarrow | \hat{\mu}_{qz} | s \uparrow s \uparrow c \downarrow \rangle. \tag{19}$$

Expectation values of the z-component of the magnetic moment operator of the strange and charm quarks are

$$\langle s \uparrow | \hat{\mu}_{sz} | s \uparrow \rangle = +\mu_s, \quad \langle s \downarrow | \hat{\mu}_{sz} | s \downarrow \rangle = -\mu_s, \quad \langle c \uparrow | \hat{\mu}_{cz} | c \uparrow \rangle = +\mu_c,$$
$$\langle c \downarrow | \hat{\mu}_{cz} | c \downarrow \rangle = -\mu_c. \tag{20}$$

Therefore, Eq. 19 becomes

$$\mu_{\Omega_c^0} = \frac{1}{6} (\mu_s - \mu_s + \mu_c) + \frac{1}{6} (-\mu_s + \mu_s + \mu_c) + \frac{4}{6} (\mu_s + \mu_s - \mu_c), \tag{21}$$

and this gives the quark model prediction for the ground-state magnetic moment of the Ω_c^0 baryon as

$$\mu_{\Omega_c^0} = \frac{4}{3} \mu_s - \frac{1}{3} \mu_c. \tag{22}$$

In the same way, we also determine an expression of the magnetic moment of the other strange singly charmed baryons, as reported in Table 10. Using the constituent quark masses from Sect. 2 and the masses of the strange singly charmed baryons from Table 2 for $J^P = \frac{1}{2}^+$, we calculate their magnetic moment and compare them with other theoretical predictions, as reported in Table 10.

Table 10 Ground-state magnetic moments of the strange singly charmed baryons (in μ_N)

Baryon	Expression	Present	[34]	[35]	[38,41]	[40]	[51]	[53]	[45]	[52]	[47,48]
Ξ_c^0	$\frac{2}{3}\mu_d + \frac{2}{3}\mu_s - \frac{1}{3}\mu_c$	−1.011	−0.96	—	—	0.192 (17)	—	0.39	−0.964	0.28	—
Ξ_c^+	$\frac{2}{3}\mu_u + \frac{2}{3}\mu_s - \frac{1}{3}\mu_c$	−0.523	—	—	—	0.235 (25)	—	0.41	0.709	0.40	—
Ω_c^0	$\frac{4}{3}\mu_s - \frac{1}{3}\mu_c$	−0.842	−0.96	—	0.85 ±0.05	−0.688 (31)	—	−0.85	−0.958	−0.90	−0.688 ±0.031
$\Xi_c(2645)^0$	$\mu_d + \mu_s + \mu_c$	−0.825	−1.43	−0.61	−1.57 ±0.06	—	−0.68 ±0.18	—	−0.688	−1.43	—
$\Xi_c(2645)^+$	$\mu_u + \mu_s + \mu_c$	−1.319	0.72	1.28	0.90 ±0.04	—	0.62 ±0.68	—	1.513	1.59	—
$\Omega_c(2770)^0$	$2\mu_s + \mu_c$	−0.560	−1.43	−0.27	−1.28 ±0.08	—	−1.68 ±0.42	—	−0.865	−0.86	−0.730 ±0.023

Table 11 The radiative decay widths (Γ_γ) of strange singly charmed baryons (in keV)

Decay	Present	[34]	[36]	[42]	[44]	[49]	[50]	[51]
$\Xi_c(2645)^0 \to \Xi_c^0 + \gamma$	0.776	1.84	0.36	–	0.30	0.908	1.318	0.66 ± 0.41
$\Xi_c(2645)^+ \to \Xi_c^+ + \gamma$	90.28	21.6	502	–	63.32	44.3	152.4	52 ± 32
$\Omega_c(2770)^0 \to \Omega_c^0 + \gamma$	3.726	0.32	4.82	0.89	2.02	1.07	1.439	–

4.3 Radiative decays

Electromagnetic transition strength of the singly charmed baryons is weaker and has not a phase space restriction than that of the pion transitions in the strong decay [4]. But some radiative decay modes contribute significantly to the total branching fractions of the singly charmed baryon. The radiative decay width can be expressed in terms of the radiative transition magnetic moments ($\mu_{B'_C \to B_c}$) in μ_N and photon energy (k) as discussed in [43,44]

$$\Gamma_\gamma = \frac{k^3}{4\pi} \frac{2}{2J+1} \frac{e}{m_p^2} \mu_{B_c \to B'_c}^2, \tag{23}$$

where m_p is the proton mass and J represents the total angular momentum of the initial baryon B_c.

The transition magnetic moment is determined by following the same procedure as we discussed in the above subsection. For the transition $\Omega_c(2770)^0 \to \Omega_c^0$, we write

$$\mu_{\Omega_c(2770)^0 \to \Omega_c^0} = \left\langle \Phi_{\mathrm{sf}_{\Omega_c(2770)^0}} \left| \hat{\mu}_{qz} \right| \Phi_{\mathrm{sf}_{\Omega_c^0}} \right\rangle; \tag{24}$$

the spin–flavor wave functions (Φ_{sf}) of $\Omega_c(2770)^0$ and Ω_c^0 states are

$$\left| \Phi_{\mathrm{sf}_{\Omega_c(2770)^0}} \right\rangle = (ssc) \cdot \left(\frac{1}{\sqrt{3}} (\uparrow\uparrow\downarrow + \uparrow\downarrow\uparrow + \downarrow\uparrow\uparrow) \right) \tag{25}$$

$$\left| \Phi_{\mathrm{sf}_{\Omega_c^0}} \right\rangle = (ssc) \cdot \left(\frac{1}{\sqrt{6}} (2\uparrow\uparrow\downarrow - \uparrow\downarrow\uparrow - \downarrow\uparrow\uparrow) \right). \tag{26}$$

Now repeating the procedure as we have done in the above subsection, this gives the transition magnetic moment (in μ_N) as

$$- \mu_{\Omega_c(2770)^0 \to \Omega_c^0} \quad 2\sqrt{\frac{2}{3}} (\mu_s - \mu_c) \quad -1.499.$$

In the same way, we determine the transition magnetic moment of the other strange singly charmed baryonic states:

$$- \mu_{\Xi_c(2645)^0 \to \Xi_c^0} \quad \sqrt{\frac{2}{3}} (\mu_d - \mu_s) \quad -0.176$$

$$- \mu_{\Xi_c(2645)^+ \to \Xi_c^+} \quad \sqrt{\frac{2}{3}} (\mu_u - \mu_s) \quad 1.864.$$

Using these radiative transition magnetic moments, the radiative decay widths are calculated (in keV). Our results are listed in Table 11 and compared with other theoretical predictions.

5 Summary

In the present study, the excited-state masses of the strange singly charmed baryons are calculated in the nonrelativistic framework of hypercentral constituent quark model (hCQM). A screened potential is used as a confining potential with the first-order correction to see the relativistic effect in the heavy–light baryonic systems. Our results are listed in Tables 2, 3, 4, 5, 6, 7 and 8 with other theoretical predictions and the available experimental measurements. Moreover, our results are plotted on Regge line according to their quantum number in both (n_r, M^2) and (J, M^2) planes as shown in Figs. 1, 2, 3, 4, 5 and 6. That help to assign the possible J^P value of the experimentally observed unknown states. Here, the spectroscopy and the Regge trajectories studies identified the states such as:

- Ξ_c baryon

the isodoublets of $\Xi_c(2970)$ and $\Xi_c(3080)$ states are assigned as a $2S$ state with $J^P = \frac{1}{2}^+$ and $\frac{3}{2}^+$, respectively; and the $\Xi_c(3123)^+$ state is predicted as a $1D$ state with $J^P = \frac{3}{2}^+$ for a spin $S = \frac{1}{2}$.

- Ω_c^0 baryon

the $\Omega_c(3000)^0$ state identified as a $1P$ state with $J^P = \frac{1}{2}^-$ and the $\Omega_c(3119)^0$ state may be $2S$ state with $J^P = \frac{1}{2}^+$.

The experimentally observed strange baryons resonances $\Xi_c(2930)$, $\Xi_c(3055)^+$, $\Omega_c(3050)^0$, $\Omega_c(3066)^0$ and $\Omega_c(3090)^0$ are not identified with their spin–parity in this work.

The strong decay rates of the isodoublet baryonic states $\Xi_c(2645)$, $\Xi_c(2790)$ and $\Xi_c(2815)$ are analyzed in the framework of heavy hadron chiral perturbation theory (HHChPT). The decays of the isodoublet $\Xi_c(2645)$ are driven by the strong coupling g_2 and h_2 controls the decays of $\Xi_c(2790)$ and $\Xi_c(2815)$ isodoublet states. Here, we used $| g_2 | = 0.550^{+0.013}_{-0.027}$ extract in our previous work [73] by using the masses from PDG-2018 [1] and $h_2 = 0.60 \pm 0.07$ was taken from the CDF collaboration [74]. Hence, using these couplings and the baryons masses from PDG-2018 [1] we update the values of their strong decay rates. Moreover, the magnetic moments and the transition magnetic moments of the ground state of strange singly charmed baryons are calculated in the constituent quark model. The radiative decay rates based on the transition magnetic moments are determined. Our results of magnetic moments and the radiative decay rates are compatible with other theoretical predictions.

The obtained mass spectra of strange singly charmed baryons are used for the study of their Regge trajectories, strong decays, magnetic moments, transition magnetic moments and radiative decay widths. This study will help experimentalists as well as theoreticians to understand the dynamics of strange singly charmed baryons. So we foresee to extend this scheme for the calculations of the strange and non-strange singly bottom baryons.

References

1. M. Tanabashi et al. (Particle Data Group), Phys. Rev. D **98**, 030001 (2018)
2. H.-X. Chen, W. Chen, X. Liu, Y.-R. Liu, S.-L. Zhu, Rep. Prog. Phys. **80**, 076201 (2017)
3. J. Sonnenschein, D. Weissman, Eur. Phys. J. C **79**, 326 (2019)
4. H.-Y. Cheng, Front. Phys. **10**(6), 101406 (2015)
5. B. Singh et al. (P̄ANDA Collaboration), Phys. Rev. D **95**, 032003 (2017)
6. B. Singh et al. (P̄ANDA Collaboration), Eur. Phys. J. A **52**, 325 (2016)

7. B. Singh et al. ($\overline{P}$ANDA Collaboration), Nucl. Phys. A **954**, 323 (2016)
8. B. Singh et al. ($\overline{P}$ANDA Collaboration), Eur. Phys. J. A **51**, 107 (2015)
9. B. Singh et al. ($\overline{P}$ANDA Collaboration), J. Phys. G **46**, 045001 (2019)
10. G. Barucca et al. ($\overline{P}$ANDA Collaboration), Eur. Phys. J. A **55**, 42 (2019)
11. B. Aubert et al. (BABAR Collaboration), Phys. Rev. D **77**, 031101(R) (2008)
12. B. Aubert et al. (BABAR Collaboration), Phys. Rev. D **77**, 012002 (2008)
13. Y. Kato et al. (Belle Collaboration), Phys. Rev. D **89**, 052003 (2014)
14. T. Lesiak et al. (Belle Collaboration), Phys. Lett. B **665**, 9 (2008)
15. Y. Kato et al. (Belle Collaboration), Phys. Rev. D **94**, 032002 (2016)
16. R. Aaij et al. (LHCb Collaboration), Phys. Rev. Lett. **118**, 182001 (2017)
17. B. Chen, K.-W. Wei, X. Liu, T. Matsuki, Eur. Phys. J. C **77**, 154 (2017)
18. Z. Shah, K. Thakkar, A.K. Rai, P.C. Vinodkumar, Eur. Phys. J A **52**, 313 (2016)
19. Z. Shah, K. Thakkar, A.K. Rai, P.C. Vinodkumar, Chin. Phys. C **40**, 123102 (2016)
20. T. Yoshida, E. Hiyama, A. Hosaka, M. Oka, K. Sadato, Phys. Rev. D **92**, 114029 (2015)
21. W. Roberts, M. Pervin, Int. J. Mod. Phys. A **23**, 2817 (2008)
22. D. Ebert, R.N. Faustov, V.O. Galkin, Phys. Rev. D **84**, 014025 (2011)
23. D. Ebert, R.N. Faustov, V.O. Galkin, Phys. Lett. B **659**, 612 (2008)
24. B. Chen, K.-W. Wei, X. Liu, T. Matsuki, Eur. Phys. J. A **51**, 82 (2015)
25. Y. Yamaguchi et al., Phys. Rev. D **91**, 034034 (2015)
26. H.-X. Chen et al., Phys. Rev. D **91**, 054034 (2015)
27. A. Valcarce, H. Garcilazo, J. Vijande, Eur. Phys. J. A **37**, 217 (2008)
28. X.-H. Guo, K.-W. Wei, X.-H. Wu, Phys. Rev. D **78**, 056005 (2008)
29. P.P. Rubio, S. Collins, G.S. Baliy, Phys. Rev. D **92**, 034504 (2015)
30. N. Mathur, R. Lewis, R.M. Woloshyn, Phys. Rev. D **66**, 014502 (2002)
31. D. Pirjol, T.M. Yan, Phys. Rev. D **56**, 5483 (1997)
32. H.-Y. Cheng, C.-K. Chua, Phys. Rev. D **75**, 014006 (2007)
33. H.-Y. Cheng, C.-K. Chua, Phys. Rev. D **92**, 074014 (2015)
34. G.-J. Wang, L. Meng, S.-L. Zhu, Phys. Rev. D **99**, 034021 (2019)
35. L. Meng, G.-J. Wang, C.-Z. Leng, Z.-W. Liu, S.-L. Zhu, Phys. Rev. D **98**, 094013 (2018)
36. N. Jiang, X.L. Chen, S.L. Zhu, Phys. Rev. D **92**, 054017 (2015)
37. J.-Y. Kim, H.-C. Kim (2019). arXiv:1902.02943 [hep-ph]
38. H.-C. Kim (2019). arXiv:1902.02944 [hep-ph]
39. Y. Kawakami, M. Harada, Phys. Rev. D **97**, 114024 (2018)
40. R.-X. Shi, Y. Xiao, L.-S. Geng (2018). arXiv:1812.07833v1 [hep-ph]
41. G.-S. Yang, H.-C. Kim, Phys. Lett. B **781**, 601 (2018)
42. K.L. Wang, Y.-X. Yao, X.-H. Zhong, Q. Zhao, Phys. Rev. D **96**, 116016 (2017)
43. K. Gandhi, Z. Shah, A.K. Rai, Eur. Phys. J. Plus **133**, 512 (2018)
44. A. Majethiya, B. Patel, P. Vinodkumar, Eur. Phys. J A **42**, 213 (2009)
45. B. Patel, A.K. Rai, P.C. Vinodkumar, J. Phys. G **35**, 065001 (2008)
46. C. Albertus, E. Hernandez, J. Nieves, J.M. Verde-Velasco, Phys. Rev. D **72**, 094022 (2005)
47. K.U. Can, G. Erkol, M. Oka, T.T. Takahashi, Phys. Rev. D **92**, 114515 (2015)
48. K.U. Can, G. Erkol, B. Isildak, M. Okab, T.T. Takahashic, JHEP **5**, 125 (2014)
49. A. Bernotas, V. Simonis, Phy. Rev. D **87**, 074016 (2013)
50. T. Aliev, M. Savci, V. Zamiralov, Mod. Phys. Lett. A **27**, 1250054 (2012)
51. T. Aliev, K. Azizi, A. Ozpineci, Nucl. Phys. B **808**, 137 (2009)
52. N. Sharma, H. Dahiya, P.K. Chatley, M. Gupta, Phys. Rev. D **81**, 073001 (2010)
53. A. Faessler et al., Phys. Rev. D **73**, 094013 (2006)
54. M.A. Ivanov, J.G. Korner, V.E. Lyubovitskij, A.G. Rusetsky, Phys. Rev. D **60**, 094002 (1999)
55. S. Tawfiq, P.J. ODonnell, J.G. Korner, Phys. Rev. D **58**, 054010 (1998)
56. C. Chen, X.L. Chen, X. Liu, W.Z. Deng, S.L. Zhu, Phys. Rev. D **75**, 094017 (2007)
57. J.-M. Richard, Phys. Rep. **212**, 1 (1992)
58. M.M. Giannini, E. Santopinto, Chin. J. Phys. **53**, 020301 (2015)
59. Z. Shah, K. Gandhi, A.K. Rai, Chin. Phys. C **43**, 024106 (2019)
60. Z. Ghalenovi, A. Rajabi, S.-X. Qin, D.H. Rischke, Mod. Phys. Lett. A **29**, 1450106 (2014)
61. N. Salehi, A. Rajabi, Z. Ghalenovi, Acta Phys. Polon. B **42**, 1247 (2011)
62. E. Santopinto, Phys. Rev. C **72**, 022201 (2005)
63. Y. Koma, M. Koma, H. Wittig, Phys. Rev. Lett. **97**, 122003 (2006)
64. J.-Z. Wang, D.-Y. Chen, X. Liu, T. Matsuki, Phys. Rev. D **99**, 114003 (2019)
65. M.B. Voloshin, Prog. Part. Nucl. Phys. **61**, 455 (2008)
66. R. Bijker, F. Iachello, A. Leviatan, Ann. Phys. (N.Y.) **236**, 69 (1994)

67. R. Bijker, F. Iachello, E. Santopinto, J. Phys. A **31**, 9041 (1998)
68. W. Lucha, F. Schoberls, Int. J. Mod. Phys. C **10**, 607 (1999)
69. J. Yelton et al. (Belle Collaboration), Phys. Rev. D **94**, 052011 (2016)
70. B. Silvestre-Brac, F. Brau, C. Semay, J. Phys. G **29**, 2685 (2003)
71. B. Aubert et al. (BABAR Collaboration), Phys. Rev. D **97**, 232001 (2006)
72. J. Yelton et al. (Belle Collaboration), Phys. Rev. D **97**, 051102 (2018)
73. K. Gandhi, Z. Shah, A. K. Rai, Communicated (2019). arXiv:1912.05859
74. T. Aaltonen et al. (CDF Collaboration), Phys. Rev. D **84**, 012003 (2011)